Langmuir

Article

pubs.acs.org/Langmuir

Synthesis and Characterization of Novel Pyrene-Dendronized Porphyrins Exhibiting Efficient Fluorescence Resonance Energy Transfer: Optical and Photophysical Properties

Gerardo Zaragoza-Galán,[†] Michael A. Fowler,[‡] Jean Duhamel,*[,‡] Regis Rein,[§] Nathalie Solladié,[§] and Ernesto Rivera*[,†]

[†]Instituto de Investigaciones en Materiales, Universidad Nacional Autónoma de México, Ciudad Universitaria, C.P. 04510 México D.F., México

[‡]Institute for Polymer Research, Waterloo Institute for Nanotechnology, Department of Chemistry, University of Waterloo, Waterloo, ON N2L 3G1, Canada

[§]Laboratoire de Chimie de Coordination du CNRS, 205 route de Narbonne 31077 Toulouse Cedex 4, France

Supporting Information

ABSTRACT: A novel series of pyrene dendronized porphyrins bearing two and four pyrenyl groups (Py_2-TMEG1 and Py_4-TMEG2) were successfully synthesized. First and second generation Fréchet type dendrons (Py_2-G1OH and Py_4-G2OH) were prepared from 1-pyrenylbutanol and 3,5-dihydroxybenzyl alcohol. These compounds were further linked to a trimesitylphenylporphyrin containing a butyric acid spacer via an esterification reaction to obtain the desired products. Dendrons and dendronized porphyrins were fully characterized by FTIR and ^{1}H NMR spectroscopy and their molecular weights were determined by matrix-assisted laser desorption ionization time of flight mass spectrometry. Their optical and photophysical properties were studied by absorption and fluorescence spectroscopies. The formation of dynamic excimers was detected in the pyrene-labeled dendrons, with more excimer being produced in the higher generation dendron. The fluorescence spectra of the pyrene dendronized porphyrins exhibited a significant decrease in the amount of pyrene monomer and excimer emission, jointly with the appearance of a new emission band at 661 nm characteristic of porphyrin emission, an indication that fluorescence resonance energy transfer (FRET) occurred from one of the excited pyrene species to the porphyrin. The FRET efficiency was found to be almost quantitative ranging between 97% and 99% depending on the construct. Model Free analysis of the fluorescence decays acquired with the pyrene monomer, excimer, and porphyrin core established that only residual pyrene excimer formation in the dendrons could occur before FRET from the excited pyrene monomer to the ground-state porphyrin core.

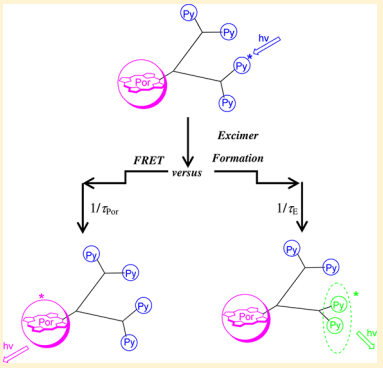

INTRODUCTION

Since their discovery, dendrimers have attracted the interest of the scientific community due to their unique chemical and physical properties.[1] Their use in photo- and electroactive devices deserves special attention because of their potential application in chemistry, medicine, and materials science.[2] The study of the photophysical properties of dendrimers is particularly interesting and is highly dependent on the complex architectures of these macromolecules. Photoactive units can be attached covalently or noncovalently to dendrimers at three different locations: periphery, branches, or core. Depending on the nature of the chromophores and their location in the dendritic structure, excimer and exciplex formation, fluorescence resonance energy transfer (FRET), and charge transfer (CT) processes may occur.[3] The knowledge derived from the study of photoactive dendrimers is significant, since it contributes to improving the efficiency of existing photovoltaic technologies.[3−6] Such considerations have led to the preparation and characterization of a large number of dendritic constructs labeled with different chromophores selected for their specific photophysical properties. Yet, among the many photoactive dendritic constructs that have been prepared to date, only a few have been studied that were covalently labeled with the widely used chromophores pyrene and porphyrin.

As a matter of fact, pyrene has been reported to be "by far the most frequently used dye in fluorescence studies of labeled polymers",[7] and its properties have been and continue to be the object of numerous reviews.[8−13] The widespread use of pyrene as a fluorescent label to characterize macromolecules of various sizes and architectures is due to its unique photophysical properties, principally its ability to form an excimer.[7−12] Pyrenyl groups have been incorporated into several macromolecular systems in order to study micelle formation,[14] polymer chain dynamics,[8−12] internal dynamics of dendrimers,[11,15] and to design novel π-conjugated pyrene-based polymers and oligomers.[16] In a seminal work, Stewart and Fox

Received: March 27, 2012
Revised: June 22, 2012
Published: June 27, 2012

reported efficient electron transfer from dimethylaniline to the lowest singlet-state pyrene and pyrene excimer in a family of dendronized structures having pyrene end groups and dimethyl aniline at the benzylic position.[17] Cicchi et al. have prepared a series of Fréchet-type dendrons whose periphery was fully decorated with pyrenyl labels via a Huisgen reaction.[18] They found that excimer formation as well as the efficiency of energy transfer from an excited pyrene to different acceptor groups scales linearly with the generation number of the dendron. In the study by Yip et al., the efficiency and average rate constant of excimer formation were determined for a series of pyrene-labeled dendrimers,[15] and both showed a linear dependence with increasing generation number. Even more recently, Vanjinathan et al. have reported the synthesis of a series of light-harvesting dendrimers containing pyrene end groups and a 2,6-(dimethyl-4H-pyran-4-ylidene) malonitrile (DCM) core.[19] They found that the efficient energy transfer that occurred from the pyrene units to the DCM core was promoted by an antenna effect induced by the dendritic structure. Surprisingly, Vanjinathan's dendrimers did not show any excimer emission even for high generations.[19]

Porphyrins are part of a very important family of fluorophores, which have been widely studied in macromolecular and materials science.[20−23] The design of new porphyrin and multiporphyrinic arrays is of great interest due to their application in catalysis,[20] nonlinear optics (NLO),[21] two photon absorption,[22] and molecular wires.[23] Several electro- and photoactive units have been incorporated into porphyrins in order to tune their electronic and photophysical properties. The donor−acceptor character of porphyrins can also be modified depending on their coordination state and the photoactive units linked to them.[24−26]

Although the preparation and properties of several porphyrin derivatives linked to electro- and photoactive units (fullerene C_{60},[24] anthracene,[25] functionalized porphyrins,[26] etc.) have been reported in the literature, only a few articles about porphyrin−pyrene systems have been published.[27] Furthermore, none of these earlier works focused on the study of light harvesting antenna effects and energy transfer properties. Since the emission of the pyrene monomer and excimer[7] partially overlap, the Soret absorption bands of porphyrins (λ = 419 nm for tetraphenyl porphyrin (TPP) and λ = 423 nm for its Zn-loaded equivalent (ZnTPP)),[28,29] efficient fluorescence resonance energy transfer (FRET) is expected to take place in macromolecular constructs labeled with porphyrin and pyrene units. Consequently, at least three distinct photophysical processes are expected to occur simultaneously in such constructs. First, excimer should be generated by the pyrenyl pendants; second and third, FRET should take place from an excited pyrenyl unit or an excimer to the porphyrin, respectively. Since dealing with a single photophysical process occurring intramolecularly inside a photoactive macromolecule is complicated to start with, dealing with three different processes simultaneously would be a photophysical nightmare. Fortunately, these photophysical processes depend strongly on molecular parameters that can be modified in a controlled manner to affect selectively the magnitude of one of the photophysical processes over the others and in turn enable the quantitative characterization of all photophysical processes. Indeed, pyrene excimer formation and FRET depend strongly on the local pyrene concentration and the distance between the energy donor (pyrene monomer and excimer) and acceptor (porphyrin), respectively.

These facts were taken into account to design two molecular constructs labeled with porphyrin and pyrene. Poly(aryl ether) dendrons of generations 1 and 2 fully labeled at the chain ends with 1-pyrenebutyl substituents were synthesized to take advantage of the enhanced excimer formation that occurs with increasing generation number for pyrene-labeled dendrimers.[15,18] The focal point of the pyrene-labeled dendrons was then connected to a porphyrin unit via a flexible spacer. Since the distance between the periphery of a dendron and its focal point increases with increasing generation number, increasing the generation number of the pyrene-labeled dendrons from 1 to 2 increased the average distance between the pyrenyl units and the porphyrin, thus reducing the FRET efficiency. Consequently, increasing the generation number of the dendron used in these constructs increased excimer formation and decreased FRET. The chemical structure of these constructs is shown in Figure 1. This report describes the

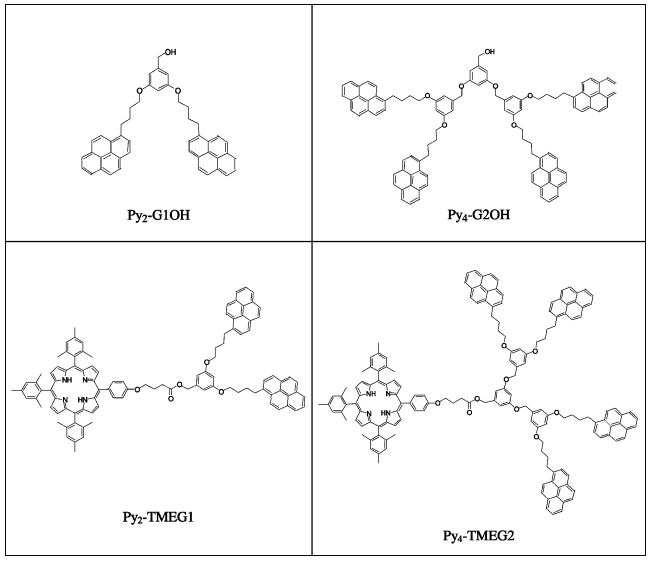

Figure 1. Pyrene-labeled constructs investigated in this work.

synthesis of these constructs as well as the effect that subtle changes made to the molecular geometry of these photoactive constructs have on the different photophysical processes at play.

EXPERIMENTAL SECTION

Chemicals. All the reagents involved in the synthesis were purchased from Aldrich and used as received. The solvents used in the reactions were purified by simple distillation. Synthesis of the pyrene−porphyrin dendritic systems is described in detail in the Supporting Information.

Instrumentation. FTIR spectra of the intermediates, dendrons, and pyrene−porphyrin dendritic systems were carried out on a Spectrum 100 (Perkin−Elmer) spectrometer in solid state. ^{1}H and ^{13}C NMR spectra of these compounds in $CDCl_3$ solution were recorded at room temperature on a Bruker Avance 400 MHz spectrometer, operating at 400 and 100 MHz for ^{1}H and ^{13}C, respectively. Matrix-assisted laser desorption ionization time of flight mass spectrometry (MALDI-TOF MS) measurements were obtained in a BRUKER Microflex spectrometer. For UV−vis and fluorescence spectroscopies, tetrahydrofuran (THF) was purchased from Aldrich (spectrophotometric grade). Prior to use, the solvent was checked for spurious emission in the region of interest and found to be satisfactory. The absorption spectra of the final compounds in solution were recorded on a Varian Cary 1 Bio UV/vis spectrophotometer using 1 cm quartz

dx.doi.org/10.1021/la301284v | Langmuir 2012, 28, 11195−11205

cells and solute concentrations of $1-3 \times 10^{-5}$ M for the dendrimer compounds. Porphyrin sample concentrations of 3×10^{-6} M and 8×10^{-5} M were used to determine the molar absorbance coefficient of the constructs at the Soret band and 344 nm, respectively. It has been verified that the Beer–Lambert law applies for the concentrations used. Fluorescence spectra corrected for the emission detection were recorded on a Photon Technology International LS-100 steady-state fluorometer having a continuous Ushio UXL-75Xe xenon arc lamp and a PTI 814 photomultiplier detection system. Each solution was excited at 344 nm using a 1 cm quartz cell. For all compounds, a pyrene concentration of less than 1.25×10^{-6} M was used to ensure that the solutions would have an absorbance of 0.05 at 344 nm in order to avoid the inner filter effect. Time-resolved fluorescence decays were acquired using an IBH Ltd. time-resolved fluorometer equipped with an IBH 340 nm NanoLED. The samples were excited at 344 nm, and the monomer, excimer, and porphyrin fluorescence decays were acquired at 375, 510, and 650 nm, respectively. Residual light scattering was blocked off from reaching the detector with cutoff filters at 370, 480, and 550 nm, respectively. The instrument response function was determined with a Ludox solution. The decays were fitted using the Model Free analysis (MF) that has been described in a number of articles. Optimization of the pre-exponential factors and decay times was accomplished with the Marquardt–Levenberg algorithm.[37] The quality of the fits was determined from the χ^2 parameter ($\chi^2 < 1.30$) and the random distribution of the residuals and the autocorrelation of the residuals. Errors on the fitted parameters were estimated by using the parameters retrieved from a given fit to simulate 10 fluorescence decays with different Poisson noise pattern. The simulated decays were fitted, the results from the fits were averaged, and the standard deviation was determined for all parameters. For most parameters retrieved from the analysis of the fluorescence decays, the error was less than 5%.

Analysis of the Fluorescence Spectra. Due to the low fluorescence intensity of the Py_2-TMEG1 and Py_4-TMEG2 samples, careful precautions were necessary to prevent contamination of the solution by pyrene, as even trace amounts of pyrene were able to significantly affect the obtained results. The fluorescence cells were cleaned with a solution of ammonium persulphate in concentrated sulphuric acid before use. Fresh solvent was used each day and checked for pyrene contamination before preparing the samples.

Degassing initially proved to be a contaminating step as trace pyrene was transferred from the rubber septum to the degassing needle and then to the sample solutions. To prevent this, rubber septa were rinsed with acetone. The needle used for degassing the solutions was pushed through the septum before being rinsed inside and out with acetone and dried with a stream of nitrogen. After cleaning, the needle was kept from contact with any surface other than clean Kimwipes until it was inserted into the fluorescence cell and the septum was sealed. After degassing, the needles were pulled out and the cell was sealed with a stopcock. This setup completely stops oxygen from the air to diffuse into the fluorescence cell and quench the fluorescence of the solution for several hours.

Before acquiring sample spectra, the THF used for preparing the solutions was first degassed and run on the spectrophotometer. This served two purposes: one being to provide a baseline spectrum of the solvent that was subtracted from all subsequent sample spectra. This was found to be especially important because the Raman scattering signal from the solvent was of comparable intensity to the sample signal (see the Supporting Information, Figure S2). The second purpose was to ensure that the solvent, the fluorescence cells, and all equipment used to prepare and degas the samples were completely pyrene free and that the contamination prevention protocol was successful.

Spectra were acquired with an excitation slit bandwidth of 4 nm and an emission slit bandwidth of 1.5 nm. The integration time per data point was increased by a factor of 5 compared to standard procedure in our laboratory, acquiring the fluorescence signal for 0.5 s/nm to improve the signal-to-noise ratio. A representative sample spectrum, with the corresponding solvent spectrum, is shown in the Supporting Information, Figure S2A. Scattering from the solvent, which would be undetected under normal conditions, induces a clear distortion of the fluorescence spectrum in the 350–365 nm wavelength range due to the Raman peak at 380 nm in the solvent spectrum. Subtraction of the solvent spectrum from the sample spectrum yields the typical fluorescence spectrum of pyrene in the Supporting Information, Figure S2B. The fluorescence spectra were acquired in triplicate to estimate the error on the reported values.

The fluorescence spectra of the constructs were then compared to the fluorescence spectrum of a 2.5×10^{-6} M solution of pyrene in cyclohexane whose fluorescence quantum yield has been reported to equal 0.32.[33] The fluorescence spectra of the constructs were then normalized to ensure that their integration over the proper range of wavelengths (360–580 nm for pyrene and 580–680 nm for porphyrin) would yield their corresponding fluorescence quantum yield.

Determination of the Förster Radius. The Förster radius for the pyrene–porphyrin donor–acceptor pair was calculated using eq 1:

$$R_o = 9790 \times (\kappa^2 \times n^{-4} \times \varphi_d \times J)^{1/6} \quad (1)$$

where R_o is the Förster radius in angstroms, κ^2 is the orientation factor set to equal $^2/_3$ assuming a random orientation of the emission and absorption dipole moments of the donor and acceptor, respectively, n is the refractive index of the solvent (1.4050 for THF), ϕ_d is the fluorescence quantum yield of the 1-pyrenebutyl donor found to equal 0.524 in Table 1, and J is the overlap integral of the pyrene–porphyrin pair.[34] The overlap integral was calculated from the fluorescence emission spectrum of 1-pyrenebutanol in THF for the donor, since excimer formation was found to be negligible due to the large rate at which FRET occurs relative to the rate of excimer formation. The molar extinction coefficients of Py_2-TMEG1 and Py_4-TMEG2 across the 1-pyrenebutanol emission spectrum were calculated. The Förster radius for each sample was determined and found to equal 5.2 nm.

Table 1. Quantum Yields and FRET Efficiency for Pyrene-Labeled Dendrons and Pyrene Dendronized Porphyrins

compound	quantum yield (Φ) pyrene units[a] (λ_{ex} = 344 nm)	quantum yield (Φ) porphyrin units[b] (λ_{ex} = 344 nm)	E_{FRET}[c]
PyBuOH (±error)[d]	0.52 (0.03)	–	–
TME (±error)[d]	–	0.0015 (0.0001)	–
Py_2-G1OH (±error)[d]	0.63 (0.02)	–	–
Py_4-G2OH (±error)[d]	0.60 (0.03)	–	–
Py_2-TMEG1 (±error)[d]	0.008 (0.001)	0.0015 (0.00005)	0.99
Py_4-TMEG2 (±error)[d]	0.018 (0.003)	0.0014 (0.0001)	0.97

[a]All reported fluorescence quantum yields were determined using the fluorescence quantum yield of pyrene in cyclohexane as a reference which has been reported to equal 0.32.[38] [b]This value is the fluorescence quantum yield of the porphyrin core having undergone FRET from an excited pyrene to the porphyrin. It is calculated by integrating the porphyrin fluorescence intensity in Figure 3 between 580 and 680 nm, after the fluorescence spectrum was correct to account for the direct excitation of porpyrin. [c]E_{FRET} is the FRET efficiency, calculated using the following equation:

$$E_{FRET} = 1 - \frac{I_{(Py+Por)}}{I_{(Py)}}$$

where $I_{(py+por)}$ is the absolute fluorescence intensity of one mole of pyrenyl pendant in a dendron and $I_{(py)}$ is the absolute fluorescence intensity of one mole of pyrene attached to the corresponding dendron. [d]All experiments were conducted in triplicate.

dx.doi.org/10.1021/la301284v | Langmuir 2012, 28, 11195–11205

RESULTS AND DISCUSSION

Synthesis of Pyrene Dendrons and Pyrene-Labeled Dendronized Porphyrins. The pyrene-labeled dendrons were prepared according to the classical convergent synthesis two-step protocol shown in Scheme S1 in the Supporting Information consisting in activation-condensation of 3,5-dialkylated-benzyl alcohol and 1-pyrenebutanol to yield the free dendrons Py_2-G1OH and Py_4-G2OH.[30] The porphyrin precursor TMA was obtained following a procedure previously reported for the preparation of tert-butyl substituted porphyrins under Lindsaý's conditions.[31] Free-base pyrene-labeled dendronized porphyrins of first and second generations were prepared via an esterification reaction using DCC as an activating agent[32] (Scheme S2 in the Supporting Information) to yield Py_2-TMEG1 and Py_4-TMEG2, which were characterized by FT-IR, ^{1}H NMR, ^{13}C NMR, and UV−vis spectroscopy. ^{1}H NMR spectrum and proton assignment of the Py_4-TMEG2 construct are shown in Figure S1 in the Supporting Information. The molecular structure was further confirmed unambigously by MALDI-TOF MS using α-cyano-4-hydroxycinamic acid as matrix. Details of the reaction conditions and purification methods are presented in the Supporting Information. The chemical structures of Py_2-G1OH, Py_4-G2OH, Py_2-TMEG1, and Py_4-TMEG2 are given in Figure 1.

Absorption Spectra of the Pyrene−Porphyrin Dendritic Systems. Absorption spectra of the pyrene-labeled dendrons (Py_2-G1OH and Py_4-G2OH) and dendronized porphyrins (Py_2-TMEG1 and Py_4-TMEG2) are shown in Figures 2 and 3, respectively. The spectra of the pyrene-containing dendrons exhibit similar features as other pyrene compounds with a maximun absorption wavelength at λ = 344 nm, corresponding to the $S_0 \rightarrow S_2$ transition of pyrene.[7,11,12] Py_2-TMEG1 and Py_4-TMEG2 exhibited the same absorption band, followed by the Soret band around 416 nm (λ = 414 nm for Py_2-TMEG1, and λ = 418 nm for Py_4-TMEG2) arising from the porphyrin unit. The Q bands of the porphyrin unit appear in the region situated beyond 450 nm with a cut off at λ = 700 nm. The UV−vis absorption spectra of dendronized porphyrins resemble a superposition of both pyrene and porphyrin absorption spectra, thereby suggesting that there are no significant electronic interactions between these aromatic groups. The pyrene absorbance at 344 nm does not scale with the number of pyrene groups attached to the construct due to the residual absorbance of the porphyrin, which is also present at 344 nm. The actual absorbance of the pyrenyl units is obtained by normalizing the absorption spectrum of the model compound trimesityl porphyrin ester derivative TME in THF at 420 nm, shifting the porphyrin peak by 2 or 6 nm to account for the changes in absorption induced to the porphyrin ring by modification with the pyrene-labeled dendrons, and subtracting the porphyrin absorption spectrum from that of the dendron. In so doing, the absorbance spectrum of the pyrenyl substitutents is recovered. This procedure enables one to calculate the pyrene-to-porphyrin absorbance ratio (A_{Py}(344 nm)/A_{Por}(Soret)) which was found to equal 0.18 and 0.37 for Py_2-TMEG1 and Py_4-TMEG2, respectively. The doubling of the A_{Py}/A_{Por} ratio confirms that the Py_4-TMEG2 construct contains twice as many pyrenes per porphyrin than the Py_2-TMEG1 construct, as would be expected from their chemical structure (see Figure 1). By using a molar absorbance coefficient for the 1-pyrenebutyl derivative (ε_{Py}) of 42 250 $M^{-1}\cdot cm^{-1}$ as determined experimentally from the absorption spectrum of 1-pyrenebutanol in THF, ε_{Por} for porphyrin was found to equal 463 000 (±4000) $M^{-1}\cdot cm^{-1}$. This value is reasonable as ε_{Por} for tetraphenyl porphyrin in THF has been reported to equal 470 000 $M^{-1}\cdot cm^{-1}$.[26] The fact that the absorption spectra of the porphyrin constructs are the sum of the absorption spectra of the individual pyrene and porphyrin elements constituting the constructs suggest that no interaction between pyrene and porphyrin takes place in the ground-state.

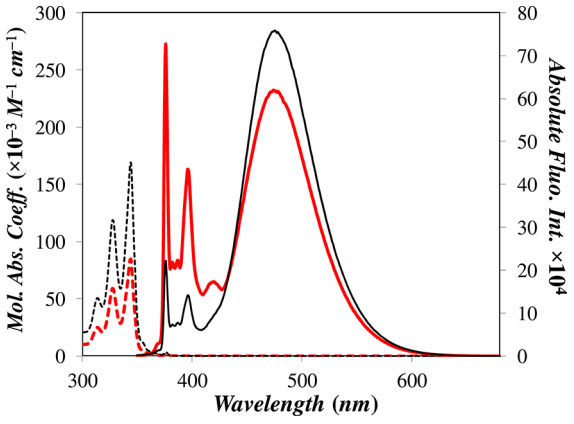

Figure 2. Absorption (dashed lines) and fluorescence (solid lines) spectra of first (Py_2-G1OH; red line) and second (Py_4-G2OH; black line) generations pyrene-labeled dendrons in THF. [Py] = 1.25 × 10^{-6} M; λ_{ex} = 344 nm.

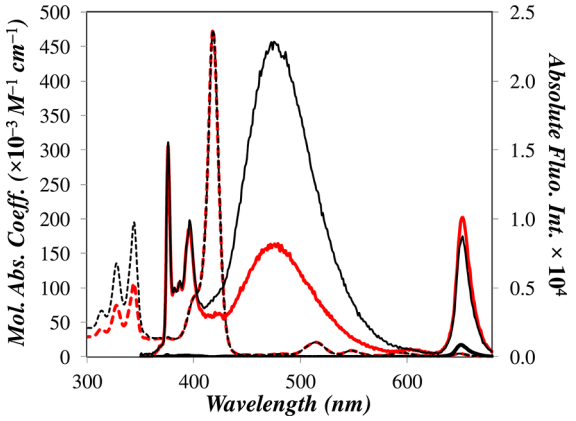

Figure 3. Absorption (dashed line) and fluorescence (solid line) spectra of Py_2-TMEG1 (red line), Py_4-TMEG2 (thin black line), and fluorescence spectrum of TME (thick black line with a low fluorescence intensity at 651 nm) in THF. [Py_2-TMEG1] = 5.1 × 10^{-7} M; [Py_4-TMEG2] = 2.6 × 10^{-7} M; and [TME] = 2.5 × 10^{-6} M; λ_{ex} = 344 nm.

Steady-State Fluorescence of the Pyrene−Porphyrin Dendritic Systems. Fluorescence spectra of compounds Py_2-G1OH and Py_4-G2OH were acquired in THF at room temperature with an excitation wavelength of 344 nm. Py_4-G2OH showed significantly more excimer emission and less monomer emission due to the increased local pyrene concentration. The fluorescence emission spectra were processed so that the reported fluorescence intensity was an absolute fluorescence intensity as integration of the fluorescence spectra in Figures 2 and 3 as a function of wavelength yields the fluorescence quantum yield of the dendrons listed in Table 1. The steady-state emission spectra show the character-

dx.doi.org/10.1021/la301284v | Langmuir 2012, 28, 11195−11205

istic pyrene monomer emission, followed by a broad excimer emission band centered at 478 nm. The excimer emission intensity (I_E) relative to that of the monomer emission (I_M), namely, the I_E/I_M ratio, increases with the number of pyrene groups in the construct from 0.69 for Py_2-G1OH to 3.05 for Py_4-G2OH. This latter trend agrees with the behavior of at least two other pyrene-labeled dendrimers, where an increase of generation number resulted in an increase in the excimer emission.[15,18] The excitation spectra recorded at the fluorescence wavelength of the monomer and excimer overlapped after normalization for both Py_2-G1OH and Py_4-G2OH. This observation indicates that the excimer and the excited monomer are the result of the excitation of a same species, namely, the pyrene monomer. When this is the case, the excimer is said to be dynamic in nature as excimer formation results from the dynamic encounter between a ground-state pyrene and an excited pyrene after excitation of a pyrene is completed.[7] When different excitation spectra are obtained, the pyrene excimer is generated via excitation of a species other than the pyrene monomer, typically a pyrene aggregate. Since excimer formation occurs via direct excitation of the pyrene aggregate without motion of the pyrene moieties in the latter case, the excimer is said to be static in nature.[7] The nature of the excimers for Py_2-G1OH and Py_4-G2OH appears to be dynamic, since the excitation fluorescence spectra of the pyrene monomer and excimer acquired at 398 and 478 nm, respectively, overlapped for both constructs.[7]

Emission spectra of the dendronized porphyrins Py_2-TMEG1 and Py_4-TMEG2 recorded with an excitation wavelength of 344 nm in THF at room temperature are shown in Figure 3. Again, the fluorescence spectra of the dendrons are presented in terms of absolute fluorescence intensity. The fluorescence features of Py_2-TMEG1 and Py_4-TMEG2 are similar to those of the pyrene-labeled dendrons, which show characteristic monomer emission at 376 nm and excimer emission at 476 nm. However, a new band appears at 651 nm corresponding to the porphyrin emission. I_E/I_M ratios of 0.58 and 1.46 were measured for Py_2-TMEG1 and Py_4-TMEG2, respectively, down from the values of 0.69 and 3.05 obtained for Py_2-G1OH and Py_4-G2OH, respectively.

Changes in the I_E/I_M ratios of these constructs can be due to a number of photophysical processes, but the most likely cause for these changes is, in our view, the presence of residual amounts of fluorescent impurities. Time-resolved fluorescence experiments described later in this report indicate that quenching of the pyrene fluorescence occurs with an average energy transfer rate constant of 2.3 and 1.8×10^9 s^{-1} for Py_2-TMEG1 and Py_4-TMEG2, respectively. Such large rate constants reflect a very efficient quenching mechanism, as illustrated by the extremely weak signal of the uncorrected fluorescence spectra obtained for Py_2-TMEG1 and Py_4-TMEG2 (see Figure S2A in the Supporting Information). As some of us have demonstrated with pyrene-labeled dendrimers, the presence of minute amounts of free label has a dramatic effect on the I_E/I_M ratio when the pyrene monomer is strongly quenched,[11,15,33] as it is the case for Py_2-TMEG1 and Py_4-TMEG2.

Whatever the variation in the I_E/I_M ratio might be, a more than 30-fold decrease in fluorescence intensity is observed when the dendrons are covalently linked to the porphyrin, a result of the highly efficient FRET taking place from an excited pyrene monomer or excimer to the porphyrin. Indeed, pyrene fluorescence of Py_2-TMEG1 and Py_4-TMEG2 is quenched almost quantitatively (99% and 97%, respectively) as reported in Table 1.

Quenching of the pyrene fluorescence in the Py_2-TMEG1 and Py_4-TMEG2 constructs is accompanied by the appearance of a new emission band at 651 nm arising from the porphyrin unit. This emission is much larger than that obtained by the direct excitation of a TME solution having the same absorption at 344 nm as that contributed by the porphyrin core in the Py_2-TMEG1 and Py_4-TMEG2 solution shown in Figure 3. The marked decrease of the fluorescence of the donor (pyrene monomer and excimer) together with the enhancement in the fluorescence intensity of the acceptor (porphyrin) is a clear signature that FRET is taking place in the pyrene−porphyrin dendritic systems Py_2-TMEG1 and Py_4-TMEG2.[34] The fluorescence spectra shown in Figure 3 corrected for the contribution from the porphyrin directly excited at 344 nm were used to determine the fluorescence quantum yield of the porphyrin core of the constructs. After averaging for Py_2-TMEG1 and Py_4-TMEG2, the porphyrin quantum yield was found to equal $1.45\ (\pm 0.1) \times 10^{-3}$. Within experimental error, it is equal to the fluorescence quantum yield of $1.5\ (\pm 0.1) \times 10^{-3}$ found for the porphyrin model compound TME, which suggests that almost all the energy absorbed by pyrene after excitation at 344 nm is transferred with hardly any loss to the porphyrin core of the dendrons. This statement is further supported when the FRET efficiency (E_{FRET}) is calculated from the fluorescence spectra shown in Figures 2 and 3. E_{FRET} values listed in Table 1 are almost equal to unity, suggesting full transfer of energy from the excited pyrene monomer and excimer to the porphyrin core.

A decrease in FRET efficiency is expected based on the molecular architecture of Py_2-TMEG1 and Py_4-TMEG2 due to an increase in the donor (pyrene) to acceptor (porphyrin) distance (d_{Py-Por}) from the former construct to the latter one. However such a change could only be detected by FRET if the change in distance caused d_{Py-Por} to cross the Förster radius (R_o) threshold.[34] The massive FRET efficiency seen in both samples implies that both the pyrene and porphyrin units are well within R_o determined to equal 5.2 nm. The validity of this hypothesis was confirmed by conducting molecular mechanics optimizations using the program Hyperchem to estimate the longest distance separating pyrene from the porphyrin core in a fully stretched conformation of the constructs (see Table S1 in the Supporting Information). That distance represents a worse case scenario as the constructs are not expected to remain fully stretched in solution but rather adopt a more coiled conformation. Nevertheless, it was found to equal 3.0 and 3.5 nm for Py_2-TMEG1 and Py_4-TMEG2, respectively, well under the 5.2 nm R_o value confirming that efficient FRET takes place in these constructs.

The ability of the pyrene-labeled dendrons to form excimer was illustrated in Figure 2 where Py_4-G2OH generates more excimer more quickly (as determined by time-resolved fluorescence measurements) than Py_2-G1OH. Since the porphyrin absorbs where the pyrene excimer emits, energy transfer from an excimer to the prophyrin core could also happen, above all for Py_4-TMEG2, which shows enhanced excimer formation. That the FRET efficiency remains the same regardless of the amount of excimer being generated by the pyrene-labeled dendrons suggests that excimer formation followed by FRET from the excimer to the porphyrin represents a minor contribution to the overall FRET process. This is supported by the time-resolved fluorescence measure-

Scheme 1. Photophysical Processes Taking Place in the Py_2-TMEG1 and Py_4-TMEG2 Constructs

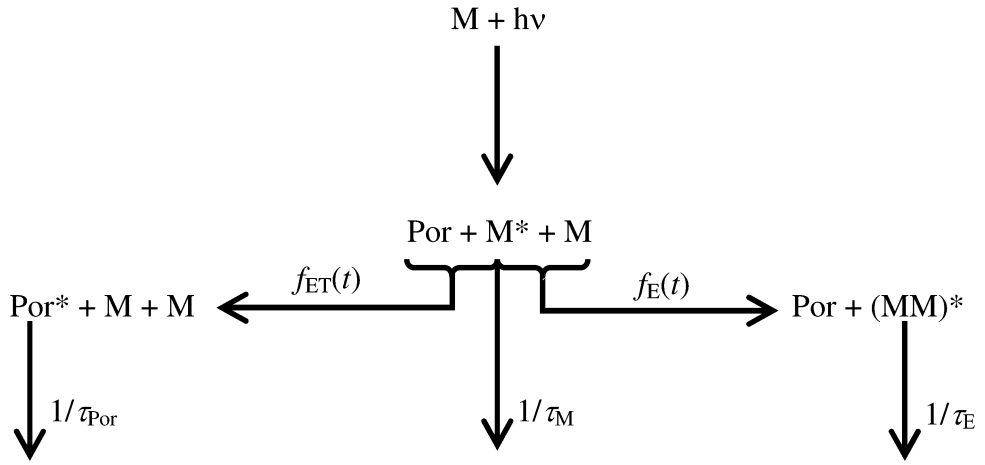

ments that indicate that FRET from the excited pyrene monomer to the porphyrin core occurs on a time scale that is more than 10 times faster than pyrene excimer formation inside the pyrene dendrons. As a first approximation, FRET between the excited pyrene monomer and porphyrin can be viewed as being so efficient that it occurs before an excimer can form. A complete description of the magnitude and time scale of the various photophysical processes at play is described hereafter through the model free (MF) analysis of the fluorescence decays acquired with the Py_2-TMEG1 and Py_4-TMEG2 constructs.

Time-Resolved Fluorescence of the Pyrene−Porphyrin Dendritic Systems. The kinetic scheme describing the photophysical processes taking place in the Py_2-TMEG1 and Py_4-TMEG2 constructs is shown in Scheme 1. Upon absorption of a photon, an excited pyrene can either form a pyrene excimer with a time-dependent rate constant $f_E(t)$ or transfer its energy to a ground-state porphyrin with a time-dependent rate constant $f_{ET}(t)$. The time-dependency of the functions $f_E(t)$ and $f_{ET}(t)$ is inferred readily from the multiexponential decays exhibited by the pyrene monomer acquired with the pyrene-labeled dendrons and the prophyrin constructs. A time-dependent rate constant $f_E(t)$ has already been observed for excimer formation in poly(2,2-bis-(hydroxymethyl)-propionic acid) dendrimers of generations 1−4 labeled with 1-pyrenebutyl groups and is due to the large number of pyrene labels crowded within the restricted geometry of the dendrimer interior that gives rise to a distribution of excimer formation rate constants.[15] Similarly, FRET depends strongly on the distance separating the donor from the acceptor.[34] The donor−acceptor pairs separated by short distances undergo efficient FRET at the early times, while the more distant donor−acceptor pairs result in less efficient FRET at longer times. Consequentl, the rate "constant" for FRET $f_{ET}(t)$ decreases with increasing time. Implicit in Scheme 1 is the assumption that no FRET occurs between a pyrene excimer and porphyrin. The validity of this assumption will be checked posteriori after analysis of the fluorescence decays acquired with the various pyrene-labeled constructs.

The time scale over which pyrene excimer formation takes place was determined by fitting the pyrene monomer and excimer fluorescence decays of Py_2-G1OH and Py_4-G2OH according to the model free (MF) analysis.[11,12,14b,15,33,35,36] The MF analysis is ideally suited to fit globally the fluorescence decays of the reactants and the products of a photophysical reaction whose kinetics are coupled when little is known about the exact expression of the rate constant describing the photophysical reaction, as is the case for pyrene excimer formation in pyrene-labeled dendrimers or FRET between an excited pyrene and a porphyrin. In the application of the MF analysis to study excimer formation in pyrene-labeled macromolecules, four pyrene species are assumed to exist when excimer formation takes place in solution.[11,12,14b,15,33,35,36] The majority of pyrene monomers form excimer by diffusion, and they are referred to as Py^*_{diff}. Despite the thorough purification protocols applied by experimentalists to remove unreacted pyrene labels, most pyrene-labeled macromolecules cannot be completely freed of unattached pyrene labels that emit with the natural lifetime of pyrene (τ_M).[11,12,15,33] These free pyrene labels are accounted for in the analysis and are referred to as Py^*_{free}. Labeling of a macromolecule with several pyrenyl moieties generates a high local pyrene concentration within the macromolecular volume that induces the formation of pyrene dimers that emit as excimer (E0*) with a lifetime τ_{E0} if properly stacked or as pyrene dimers (D*) with a lifetime τ_D if improperly stacked.

By taking advantage of the small dissociation rate constant k_{-1} usually obtained for the pyrene excimer in pyrene-labeled macromolecules,[12] the MF analysis assumes that k_{-1} equals zero.[11,12,14b,15,33,35,36] While this assumption has been found to yield reasonable results for numerous pyrene-labeled macromolecules[12] and another family of pyrene-labeled dendrons, namely, poly(2,2-bis(hydroxymethyl)-propionic acid) dendrons end-labeled with pyrene,[15] it must be pointed out that non-negligible k_{-1} values have been retrieved particularly for macromolecular constructs where pyrene excimer is formed under strained conditions, with one case in point being 1,3-di(1-pyreny)propane.[39] Larger than expected k_{-1} values were found when Birks' scheme was applied to fit the fluorescence decays acquired with pyrene-labeled macromolecules forming little excimer such as long poly(ethylene oxide) chains end-labeled with pyrene.[40] This observation was found to be a result of the breakdown of Birks' scheme under such conditions where the Fluorescence Blob Model that assumes no excimer dissociation should be applied instead. The equations used to fit the monomer and excimer fluorescence decays according to the MF analysis have been derived in a number of earlier publications,[11,12,14b,15,33,35,36] and they are given as eqs S7 and

dx.doi.org/10.1021/la301284v | Langmuir 2012, 28, 11195−11205

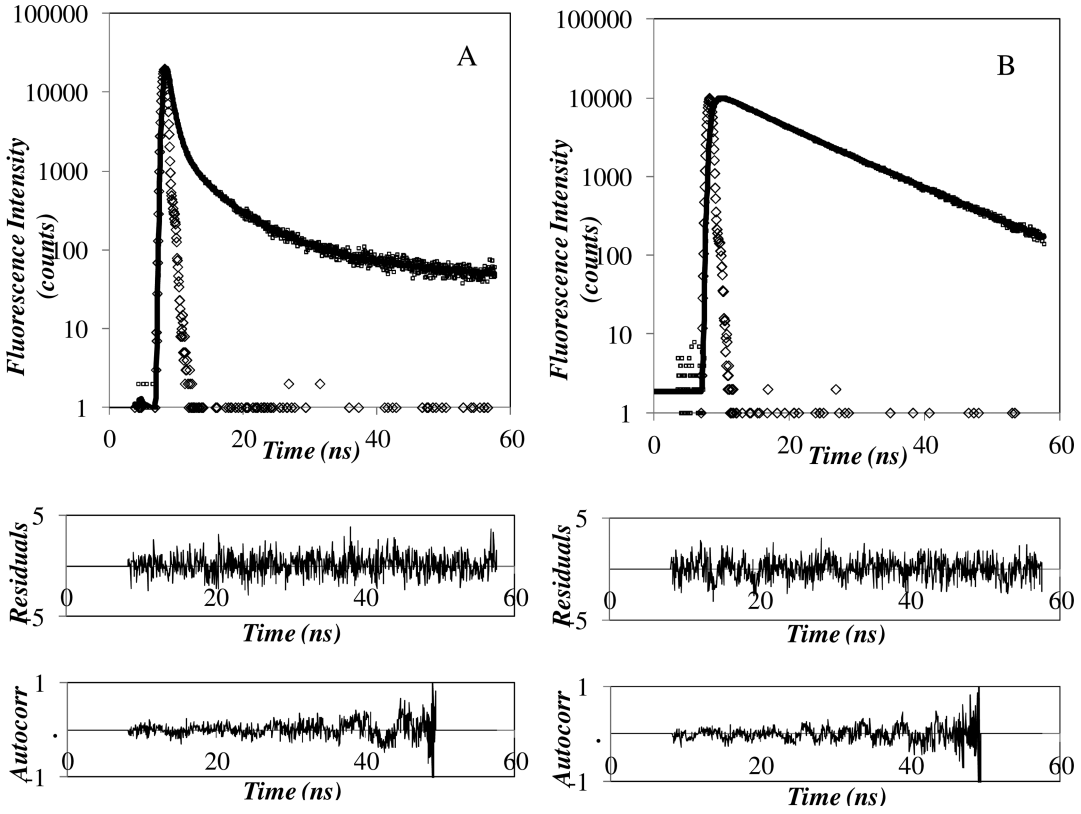

Figure 4. Global analysis of the pyrene monomer (A, λ_{em} = 375 nm) and porphyrin (B, λ_{em} = 650 nm) fluorescence decays according to eqs S9 and S10 of the Supporting Information for Py_4-TMEG2. Time per channel = 0.059 ns/ch; λ_{ex} = 344 nm; χ^2 = 1.07.

S8 in the Supporting Information. The results of the fits are shown in Figures S3 and S4 in Supporting Information, and the parameters retrieved from the fits are listed in the Supporting Information, Tables S2−S4. The good quality of the fits obtained for Py_2-G1OH and Py_4-G2OH suggests that, if pyrene excimer dissociation takes place in these pyrene-labeled dendrons, its influence to the kinetics of pyrene excimer formation must be small as the MF analysis assumes a k_{-1} value of zero.

Whereas the fluorescence decays of Py_2-G1OH could be fitted by assuming the existence of a single excited pyrene dimer, two excited pyrene dimers E0* and D* were found from the MF analysis of the fluorescence decays acquired with Py_4-G2OH, probably due to the larger number of pyrene labels sequestered in the small volume of the second generation dendron. Pyrene excimer formation was found to occur essentially by diffusion, with a fraction ${}^{F}f_{diff}$ of pyrene pendants forming excimer by diffusion being close to unity and equal to 0.92 and 0.97 for Py_2-G1OH and Py_4-G2OH, respectively. This result agrees with the overlapping excitation spectra obtained for the pyrene and excimer of the pyrene-labeled dendrons, which inferred the absence of pyrene dimers. These are important results as they demonstrate that very little pyrene dimer exists in the solution despite the large local pyrene concentration. These results led to the conclusion that, in the Py_2-G1OH and Py_4-G2OH dendrons, an excimer is generated overwhelmingly via the diffusive encounter between two pyrene pendants which occurs over a time scale that can be characterized from the rate constant of pyrene excimer formation. Based on the MF analysis of the monomer and excimer fluorescence decays described in the Supporting Information, the average rate constant of pyrene excimer formation by diffusion $\langle k_E \rangle$ was found to equal 3.2 and 11.2 × 10^7 s^{-1} for Py_2-G1OH and Py_4-G2OH, respectively. These $\langle k_E \rangle$ values are rather larger than the values of less than 3 × 10^7 s^{-1} typically obtained for linear polymers end-labeled or randomly labeled with pyrene.[36] However, larger $\langle k_E \rangle$ values have been obtained for excimer formation in pyrene-labeled gemini surfactant micelles[14b] and poly(2,2-bis(hydroxymethyl)-propionic acid) dendrimers of generations 1−4 labeled with 1-pyrenebutyl groups.[15] In these two latter examples, the local pyrene concentration was larger and the microenvironment more flexible than those found with the Py_2-G1OH and Py_4-G2OH dendrons thus resulting in larger $\langle k_E \rangle$ values. The increased number of pyrenyl pendants in the Py_4-G2OH dendron resulted in a 3.5-fold increase in $\langle k_E \rangle$. As will be shown hereafter, the rapid pyrene excimer formation taking place in Py_2-G1OH and Py_4-G2OH occurs on a time scale that is much slower than that of FRET between an excited pyrene monomer and a porphyrin in Py_2-TMEG1 and Py_4-TMEG2.

To reach this conclusion, the fluorescence decays of the pyrene monomer and porphyrin were acquired for the Py_2-TMEG1 and Py_4-TMEG2 constructs and fitted globally according to the MF analysis. This study represents the first example in the literature where the MF analysis is applied to probe FRET occurring intramolecularly inside a macromolecular construct. Theoretically, the process of FRET occurring between a donor and acceptor molecules tied to a macromolecule and diffusing in solution can be described quantitatively by averaging the local concentration of acceptor concentration at different time intervals along the fluorescence decay of the donor. However, this procedure still requires a mathematical equation describing the diffusive motions undergone by the donor and acceptor, which in the case of Py_2-

dx.doi.org/10.1021/la301284v | Langmuir 2012, 28, 11195−11205

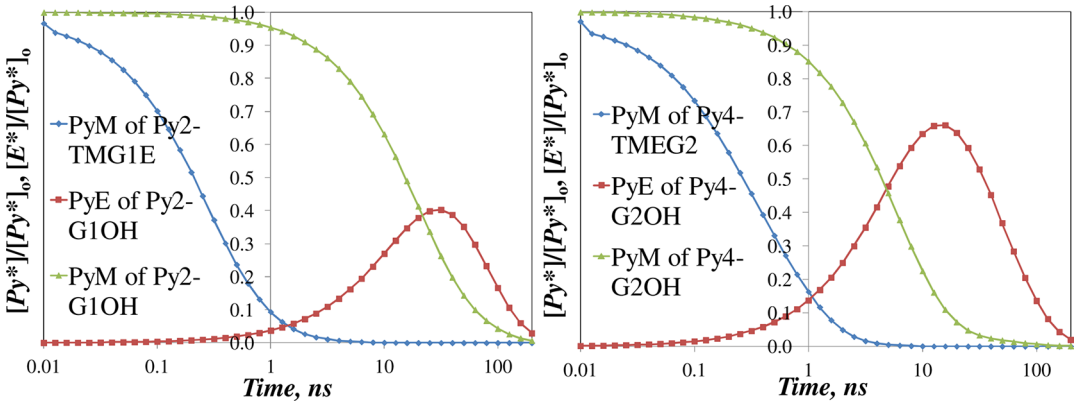

Figure 5. Fluorescence decays of the pyrene excimer (red squares) and monomer (green triangles) in the pyrene-labeled dendrons and the pyrene monomer in the porphyrin constructs (blue diamonds). Left: constructs based on Py_2-G1OH; Right: constructs based on Py_4-G2OH.

TMEG1 and Py_4-TMEG2 is not known. The MF analysis is well suited to address such cases, as it requires no prior knowledge about the mathematical details used to describe the FRET process.[11,12,14b,15,33,35,36] The equations used to fit the fluorescence decays were derived in the same manner as those used to describe the process of pyrene excimer formation. They are given as eqs S9 and S10 in the Supporting Information. The parameters describing the fluorescence decay of the directly excited porphyrins were obtained by acquiring and fitting the fluorescence decays of Py_2-TMEG1 and Py_4-TMEG2 using an excitation wavelength of 365 nm where pyrene does not absorb. When Py_2-TMEG1 was excited directly at 365 nm, the porphyrin was found to decay biexponentially with two decay times of 8 and 12 ns obtained with pre-exponential factors of 0.43 and 0.57, respectively. Under the same conditions, Py_4-TMEG2 yielded decay times of 9 and 13 ns with pre-exponential factors of 0.27 and 0.73 on direct excitation. These biexponential decays for porphyrins could indicate that porphyrin aggregates are being formed with the shorter and longer lifetimes corresponding to the aggregated and unaggregated porphyrins, respectively. They could also be a result of the modification of the porphyrin ring in one location that would result in two different porphyrin conformations. Whatever the origin of the biexponential decay, it was accounted for by considering that the pyrene labels would undergo FRET to each porphyrin species. Analysis of the parameters retrieved from the global analysis of the pyrene monomer and porphyrin fluorescence decays acquired with Py_2-TMEG1 and Py_4-TMEG2 suggests that these assumptions are realistic. The analyzed decays for Py_4-TMEG2 are shown in Figure 4.

FRET was found to occur on a fast time scale in the Py_2-TMEG1 and Py_4-TMEG2 constructs, and the decay times obtained for the pyrene monomer decays were found to match the fast rise time in the porphyrin decay suggesting that the decay of the pyrene monomer is coupled to the rise time of the porphyrin fluorescence decay. Some residual longer-lived emission in the pyrene fluorescence decays was attributed to the presence of small amounts of pyrene-labeled dendrons Py_2-G1OH or Py_4-G2OH and free pyrene labels that would not undergo FRET, either because they were not covalently attached to the porphyrin or because the porphyrin chromophores had been photobleached. Their contribution was accounted for in the MF analysis. The fits were good with residuals and autocorrelation function of the residuals randomly distributed around zero. Examples of the fluorescence decays of the pyrene monomer and porphyrin fitted with, respectively, eqs S9 and S10 are shown in Figure S5 of the Supporting Information and Figure 4 for Py_2-TMEG1 and Py_4-TMEG2, respectively. When doing these fits, the function $f_{ET}(t)$ in Scheme S5 of the Supporting Information describing FRET from the excited pyrene to the porphyrin is mathematically forced in the analysis program to be the same in accounting for the decay of the excited pyrene monomer and the rise time in the fluorescence decay of the porphyrin, in effect assuming that all excited pyrenes transfer their excess energy to porphyrin and do not form excimer. The goodness of the fits suggests that this assumption is reasonable.

As mentioned in the Supporting Information, the MF analysis of the fluorescence decays based on eqs S9 and S10 of the Supporting Information does not yield the molar fractions $f_{ET} = [Py^*_{ET}]_{(t=0)}/([Py^*_{ET}]_{(t=0)} + [Por^*]_{(t=0)})$ and $f_{Por} = [Por^*]_{(t=0)}/([Py^*_{ET}]_{(t=0)} + [Por^*]_{(t=0)})$ representing, respectively, the excited pyrenes transferring their excess energy to the porphyrin via FRET and the porphyrins directly excited at 344 nm, but rather the fraction of excitation light being absorbed by each species in solution, namely, the ratios ${}^{F}f_{ET} = \varepsilon_{Py}(344\ nm)[Py^*_{ET}]_{(t=0)}/(\varepsilon_{Py}(344\ nm)[Py^*_{ET}]_{(t=0)} + \varepsilon_{Por}(344\ nm)[Por^*]_{(t=0)})$ and ${}^{F}f_{Por} = \varepsilon_{Por}(344\ nm)[Py^*_{ET}]_{(t=0)}/(\varepsilon_{Py}(344\ nm)[Py^*_{ET}]_{(t=0)} + \varepsilon_{Por}(344\ nm)\ [Por^*]_{(t=0)})$. In turn, knowledge of the molar absorbance coefficient of pyrene (42 250 $M^{-1}\cdot cm^{-1}$) and porphyrin (19 060 $M^{-1}\cdot cm^{-1}$) at the excitation wavelength of 344 nm yields the molar fractions f_{ET} and f_{Por} from ${}^{F}f_{ET}$ and ${}^{F}f_{Por}$. The molar fractions of the various chromophore species in solution are listed in Table S8 in the Supporting Information.

The molar fractions f_{ET} and f_{Por} listed in Table S8 of the Supporting Information and recovered from the analysis of the fluorescence decays represent the molar fraction of pyrenes undergoing FRET toward the porphyrin and the molar fraction of porphyrin that are excited directly in the solution, respectively. Their values are consistent with the expected chemical composition of Py_2-TMEG1 and Py_4-TMEG2 with the latter construct containing four pyrene labels for one porphyrin (f_{ET}/f_{Por} = 0.80 (±0.03)/0.18 (±0.03) = 4.4 (±0.8) ~ 4) and the former construct containing two pyrene labels for one porphyrin (f_{ET}/f_{Por} = 0.63 (±0.01)/0.36 (±0.01) = 1.8 (±0.06) ~ 2). The good agreement obtained between the pyrene and porphyrin molar fractions retrieved from the analysis of the fluorescence decays and the actual chemical composition of the porphyrin constructs suggests that despite its limitations, Scheme 1 upon which the MF analysis is based

dx.doi.org/10.1021/la301284v | Langmuir 2012, 28, 11195−11205

provides a decent depiction of the photophysical processes at play.

One of the advantages associated with the MF analysis is that it enables one to differentiate between the different chromophore species contributing to the fluorescence decays. In particular, the parameters retrieved from the MF analysis can be used to back calculate the fluorescence decay of the pyrene monomer species forming excimer in the pyrene-labeled dendrons (Py^*_{diff}) and the pyrene excimer (E*) or the fluorescence decay of the pyrene monomer in the porphyrin constructs (Py^*_{ET}) free of any unwanted signal due to photobleached porphyrin constructs (Py^*_{den}) or unattached pyrene labels (Py^*_{free}). The result of these calculations is shown in Figure 5 using a logarithmic scale for time to better visualize the processes that occur at very early times.

According to the traces shown in Figure 5, the pyrene monomer of Py_2-TMEG1 has decayed to 2.7% of its original value after 2 ns. By that time, the pyrene monomer of Py_2-G1OH has decayed by less than 10% due to excimer formation. This observation leads to the conclusion that there remains hardly any excited pyrene in Py_2-TMEG1 to form excimer by the time excimer formation can take place. Thus, the assumption made in Scheme 1 that FRET takes place between an excited pyrene monomer and porphyrin before excimer formation occurs is well justified for Py_2-TMEG1. As expected from the chemical structure of Py_4-TMEG2, this conclusion is not as clear cut, since the higher local concentration of pyrene leads to faster excimer formation whereas the longer distance between pyrene and porphyrin results in slower FRET. The effect is well illustrated in Figure 5 where, after 1 ns, the pyrene monomer of Py_4-TMEG2 has decayed to just 16% of its original value while the pyrene monomer of Py_4-G2OH has decreased by 15%. These results suggest that some excimer formation takes place during the decay of the pyrene monomer of Py_4-TMEG2. However, the trends shown in Figure 5 for Py_4-TMEG2 still imply that a large fraction of the pyrene monomers of Py_4-TMEG2 undergo FRET before forming excimer. This point is further supported by the good fit obtained in Figure 4 where the MF analysis imposes that quenching of the pyrene monomer leads to porphyrin emission via FRET. Such a good fit would not be expected if pyrene excimer formation represented a major pathway in the quenching of the pyrene monomer. The trends obtained in Figure 5 nicely illustrate how the chemical structure of the porphyrin constructs can be adjusted to favor one photophysical process over another. Using the second generation Py_4-G2OH dendron in the Py_4-TMEG2 construct results in increased excimer formation and reduced FRET when compared to Py_2-TMEG1 as the local pyrene concentration is increased (Figure 1), and the pyrene moieties are held further away from the porphyrin core (Supporting Information, Table S1), respectively.

The average rate constant of FRET $\langle k_{ET} \rangle$ could be determined from the data listed in Table S5 of the Supporting Information and was found to equal 2.3 and 1.8×10^9 s^{-1} for Py_2-TMEG1 and Py_4-TMEG2, respectively. The smaller rate constant obtained for Py_4-TMEG2 is expected as the pyrene and porphyrin chromophores are separated by a longer distance in Py_4-TMEG2 compared to Py_2-TMEG1 (see the Supporting Information, Table S1). These $\langle k_{ET} \rangle$ values are at least 10 times larger than the largest $\langle k_E \rangle$ value of 11.2×10^7 s^{-1} obtained for Py_4-TMEG2, suggesting, along with the trends shown in Figure 5, that FRET is much likelier to take place between an excited pyrene and a porphyrin before excimer formation has time to occur.

CONCLUSIONS

A new family of pyrene-dendronized porphyrins bearing 2 and 4 pyrene moieties was successfully synthesized and characterized by a combination of techniques. Despite the large local pyrene concentration inside the pyrene-labeled constructs, no indication of the existence of ground-state pyrene dimers could be detected, either from steady-state fluorescence excitation spectra of the pyrene monomer and excimer, absorption spectra, and MF analysis of the fluorescence decays, indicating that pyrene excimer formation is dynamic in nature. Regarding the pyrene-labeled dendrons Py_2-G1OH and Py_4-G2OH, the I_E/I_M ratio was found to increase with the number of pyrenyl units attached to the dendron reflecting the increased local pyrene concentration. Once the porphyrin unit was attached to the dendron, a more than 10-fold decrease in the amount of pyrene monomer and excimer emission was observed. Another emission band at 661 nm appeared after excitation of the pyrene unit a 344 nm, indicating that FRET is taking place from the pyrene species (excited pyrene monomer or excimer) to the porphyrin acceptor. The FRET efficiency was found to equal 99% and 97% for Py_2-TMEG1 and Py_4-TMEG2, respectively. Since FRET is highly efficient regardless of the pyrene content of the construct, it was concluded that FRET occurs essentially from the excited pyrene monomer to the porphyrin core before a pyrene excimer can be formed. This assumption was confirmed by conducting the MF analysis of the fluorescence decays acquired with Py_2-TMEG1 and Py_4-TMEG2. Although large, the largest average rate constant of intramolecular pyrene excimer formation $\langle k_E \rangle$ was found to equal 11.2×10^7 s^{-1}, more than 10 times smaller than the smallest average rate constant for FRET $\langle k_{ET} \rangle$ of 1.8×10^9 s^{-1}. This study represents the first example where dendritic constructs have been prepared with the commonly used pyrene and porphyrin chromophores. It also marks the first time that the MF analysis of fluorescence decays typically used to describe the process of pyrene excimer formation[11,12,14b,15,33,35,36] is applied to describe FRET. It has demonstrated the highly efficient nature of the FRET process that takes place for the most part between the pyrene and porphyrin chromophores and how the various photophysical processes taking place in the constructs were individually characterized by steady-state and time-resolved fluorescence, thus providing a unique description of their contribution to the overall FRET mechanism.

ASSOCIATED CONTENT

Supporting Information

Details of the synthetic methods, mathematical derivations, graphs, pre-exponential factors, decay times retrieved from the global analysis of the fluorescence decays of all fluorescent species, and further references. This material is available free of charge via the Internet at http://pubs.acs.org.

AUTHOR INFORMATION

Corresponding Author

*To whom correspondence should be addressed. (E. R.) E-mail: riverage@iim.unam.mx; phone: +5255 5622 4733; fax: +5255 5616 1201 2. (J. D.) E-mail: jduhamel@uwaterloo.ca; phone: 1-519-886-8883.

Notes

The authors declare no competing financial interest.

■ ACKNOWLEDGMENTS

We are grateful to Miguel Angel Canseco, Gerardo Cedillo, and Eréndira García for technical assistance. G.Z. and E.R. acknowledge CONACYT (Project 128788) for financial support. M.F. and J.D. thank NSERC for generous financial support for this project. N.S. and R.R. are grateful to CNRS for research funding.

■ REFERENCES

(1) (a) Tomalia, D. A.; Baker, H.; Dewald, J. R.; Hall, M.; Kallos, G.; Martin, S.; Roeck, J.; Ryder, J.; Smith, P. A new class of polymers: startbust-dendritic macromolecules. *Polym. J.* **1985**, *17*, 117−132. (b) Newkome, G. R.; Yao, Z.-Q.; Baker, G. R.; Gupta, V. K. Cascade molecules: a new approach to micelles. A [27]-arborol. *J. Org. Chem.* **1985**, *50*, 2003−2017. (c) Wörner, C.; Mülhaupt, R. Polynitrile and polyamine functional poly(trimethylene imine) dendrimers. *Angew. Chem., Int. Ed. Engl.* **1993**, *32*, 1306−1308. (d) Newkome, G. R.; Moorefield, C. N.; Vögtle, F. In *Dendritic Molecules: Concepts, Syntheses, Perspectives*; VCH: New York, 1996; (f) Tomalia, D. Birth of a new macromolecular architecture: dendrimers as quantized building blocks for nanoscale synthetic polymer chemistry. *Prog. Polym. Sci.* **2005**, *30*, 294−324.

(2) (a) Nantalaksakul, A.; Reddy, R.; Bardeen, C.; Thayumanavan, S. Light harvesting dendrimers. *Photosynth. Res.* **2006**, *87*, 133−150. (b) Ceroni, P.; Venturi, M. Photo- and electro-active dendrimers: future trends and applications. *Aust. J. Chem.* **2011**, *64*, 131−146.

(3) Ceroni, P.; Bergamini, G.; Marchioni, F.; Balzani, V. Luminiscence as a tool to investigate dendrimer properties. *Prog. Polym. Sci.* **2005**, *30*, 453−473.

(4) Adronov, A.; Fréchet, J. M. J. Light-harvesting dendrimers. *Chem. Commun.* **2000**, 1701−1710.

(5) Fréchet, M. J. Dendrimers and other dendritic macromolecules: From building blocks to functional assemblies in nanoscience and nanotechnology. *J. Polym. Sci., Part A: Polym. Chem.* **2003**, *41*, 3713−3725.

(6) Balzani, V.; Ceroni, P.; Maestri, M.; Vicinelli, V. Light-harvesting dendrimers. *Curr. Opin. Chem. Biol.* **2003**, *7*, 657−665.

(7) Winnik, F. M. Photophysics of preassociated pyrenes in aqueous polymer solutions and in other organized media. *Chem. Rev.* **1993**, *93*, 587−614.

(8) Winnik, M. A. End-to-end cyclization of polymer chains. *Acc. Chem. Res.* **1985**, *18*, 73−79.

(9) Duhamel, J. Polymer chain dynamics in solution probed with a fluorescence blob model. *Acc. Chem. Res.* **2006**, *39*, 953−960.

(10) Duhamel, J. In *Molecular Interfacial Phenomena of Polymers and Biopolymers*; Chen, P., Ed.; Woodhead Publishing Company: Cambridge, U.K., 2005; pp 214−248.

(11) Duhamel, J. Internal dynamics of dendritic molecules probed by pyrene excimer formation. *Polymers* **2012**, *4*, 211−239.

(12) Duhamel, J. New insights in the study of pyrene excimer fluorescence to characterize macromolecules and their supramolecular assemblies in solution. *Langmuir* **2012**, *28*, 6527−6538.

(13) Figueira-Duarte, T. M.; Müllen, K. Pyrene-based materials for organic electronics. *Chem. Rev.* **2011**, *111*, 7260−7314.

(14) (a) Ogawa, M.; Momotake, A.; Arai, T. Water-soluble dendrimers as a potential fluorescence detergent to form novel micelles at very low CMC. *Tetrahedron Lett.* **2004**, *45*, 8515−8518. (b) Keyes-Baig, C.; Duhamel, J.; Wettig, S. Characterization of the behavior of a pyrene substituted gemini surfactant in water by fluorescence. *Langmuir* **2011**, *27*, 3361−3371.

(15) Yip, J.; Duhamel, J.; Bahun, G. J.; Adronov, A. A study of the dynamics of the branch ends of a series of pyrene-labeled dendrimers based on pyrene excimer formation. *J. Phys. Chem. B* **2010**, *114*, 10254−10265.

(16) (a) Rivera, E.; Belletete, M.; Zhu, X. X.; Durocher, G.; Giasson, R. Novel polyacetylenes containing pendant 1-pyrenyl groups: synthesis, characterization, and thermal and optical properties. *Polymer* **2002**, *43*, 5059−5068. (b) Rivera, E.; Aguilar-Martínez, M.; Terán, G.; Flores, R. F.; Bautista-Martínez, J. A. Thermal, optical and electrochemical properties of trans and the cis-poly(1-ethynylpyrene). *Polymer* **2005**, *46*, 4789−4798. (c) Illescas, J.; Caicedo, C.; Zaragoza-Galán, G.; Ramírez-Fuentes, Y. S.; Gelover-Santiago, A.; Rivera, E. Synthesis, characterization, optical and photophysical properties of novel well defined di(1-ethynylpyrenes)s. *Synth. Met.* **2011**, *161*, 775−782.

(17) Stewart, G. M.; Fox, M. A. Chromophore-labeled dendrons as light harvesting antennae. *J. Am. Chem. Soc.* **1996**, *118*, 4354−4360.

(18) Cicchi, S.; Fabbrizzi, P.; Ghini, G.; Brandi, A.; Foggi, P.; Marcelli, A.; Righini, R.; Botta, C. Pyrene-excimers-based antenna systems. *Chem.—Eur. J.* **2009**, *15*, 754−764.

(19) Vanjinathan, M.; Lin, H.-C.; Nasar, A. S. Synthesis, characterization and photophysical properties of DCM-based light-harvesting dendrimers. *Macromol. Chem. Phys.* **2011**, *212*, 849−859.

(20) Gebbink, R. J.; Suijkerbuijk, B. J. Merging porphyrins with organometallics: Synthesis and applications. *Angew. Chem., Int. Ed.* **2008**, *47*, 7396−7421.

(21) Senge, M. O.; Fazekas, M.; Notaras, E. G.; Blau, W. J.; Zawadzka, M.; Locos, O. B.; Mhuircheartaigh, E. N. Nonlinear optical properties of porphyrins. *Adv. Mater.* **2007**, *19*, 2737−2774.

(22) Pawlicki, M.; Collins, H. A.; Denning, R. G.; Anderson, H. L. Two-photon absorption and the design of two-photon dyes. *Angew. Chem., Int. Ed.* **2009**, *48*, 3244−3266.

(23) Anderson, H. L. Building molecular wires from the colors of life: conjugated porphyrin oligomers. *Chem. Commun.* **1999**, 2323−2330.

(24) Camps, X.; Dietel, E.; Hirsch, A.; Pyo, S.; Echegoyen, L.; Hackbarth, S.; Röder, B. Globular dendrimers invilving a C60 core and a tetraphenyl porphyrin function. *Chem.—Eur. J.* **1999**, *5*, 2362−2373.

(25) (a) Brettar, J.; Gisselbrecht, J.-P.; Gross, M.; Solladié, N. Tweesers hosts for intercalation of Lewis base guests: Tuning physicochemical properties of cofacial porphyrin dimers. *Chem. Commun.* **2001**, 733−734. (b) Flamigni, L.; Talarico, A. M.; Ventura, B.; Rein, R.; Solladié, N. A versatile bis-porphyrin tweezer host for the assembly of noncovalent photoactive architectures: a photophysical characterization of the tweezers and their association with porphyrins and other guests. *Chem.—Eur. J.* **2006**, *12*, 701−712.

(26) Bell, T. M.; Bhosale, S. V.; Ghiggino, K. P.; Langford, S. J.; Woodard, C. P. Synthesis and photophysical properties of a conformationally flexible mixed porphyrin star-pentamer. *Aust. J. Chem.* **2009**, *62*, 692−699.

(27) (a) Knör, G. Intramolecular charge transfer excitation of mesotetrakis (1-pyrenil)pohyrinato gold (III) acetate. Photosensitized oxidation of guanine. *Inorg. Chem. Commun.* **2001**, *4*, 160−163. (b) Sheng, N.; Sun, J.; Bian, Y.; Jiang, J.; Xu, D. Synthesis and third-order nonlinear optical properties of novel ethynyl-linked heteropentamer composed of four porphyrins and one pyrene. *J. Porphyrins Phthalocyanines* **2009**, *13*, 275−282. (c) Zhu, M.; Lu, Y.; Du, Y.; Li, J.; Wang, X.; Yang, P. Photocatalytic hydrogen evolution without an electron mediator using a porphyrin-pyrene conjugated functionalized Pt nanocomposite as photocatalyst. *J. Hydrogen Energy* **2011**, *36*, 4298−4304.

(28) Kim, J. B.; Leonard, J. J.; Longo, F. R. Mechanistic study of the synthesis and spectral of meso-tetrarylporphyrins. *J. Am. Chem. Soc.* **1972**, *94*, 3986−3992.

(29) Quimby, D. J.; Longo, F. R. Luminescence studies on sevral tetraarylporphyrins and their zinc derivatives. *J. Am. Chem. Soc.* **1975**, *97*, 5111−5117.

(30) (a) Hawker, C.; Fréchet, J. M. A new convergent approach to monodisperse dendritic macromolecules. *J. Chem. Soc., Chem. Commun.* **1990**, 1010−1013. (b) Hawker, C.; Fréchet, J. M. Preparation of polymers with controlled molecular architecture. A new convergent approach to dendritic macromolecules. *J. Am. Chem. Soc.* **1990**, *112*, 7638−7647.

(31) Solladié, N.; Hamel, A.; Gross, M. Synthesis of multiporphyrinic α-polypeptides: towards the study of the migration of an excited state for the mimicking of the natural light harvesting device. *Tetrahedron Lett.* **2000**, *41*, 6075−6078.
(32) Sheikh, M. C.; Takagi, S.; Yoshimura, T.; Morita, H. Mechanistic studies of DCC/HOBt-mediated reaction of 3-phenylpropionic acid with alcohol and studies on the reactivities of "active ester" and the related derivatives with nucleophiles. *Tetrahedron* **2010**, *66*, 7272−7278.
(33) Chen, S.; Duhamel, J.; Bahun, G.; Adronov, A. Quantifying the presence of unwanted fluorescent species in the study of pyrene-labeled macromolecules. *J. Phys. Chem. B* **2011**, *115*, 9921−9929.
(34) Lakowicz, J. R. *Principles of Fluorescence Spectroscopy*, 3rd ed.; Springer: New York, 2006.
(35) Siu, H.; Duhamel, J. Comparison of the association level of a pyrene-labelled associative polymer obtained from an analysis based on two different models. *J. Phys. Chem. B* **2005**, *109*, 1770−1780.
(36) Fowler, M.; Duhamel, J.; manuscript in preparation.
(37) Press, W. H.; Flannery, B. P.; Teukolsky, S. A.; Vetterling, W. T. *Numerical Recipes. The Art of Scientific Computing (Fortran Version)*; Cambridge University Press: Cambridge, U.K., 1992.
(38) Berlman, I. B. *Handbook of Fluorescence Spectra of Aromatic Molecules*; Academic Press: New York, 1971.
(39) Zachariasse, K. A.; Busse, R.; Duveneck, G.; Kühnle, W. Intramolecular monomer and excimer fluorescence with dipyrenylpropanes: double-exponential versus triple-exponential decays. *J. Photochem.* **1985**, *28*, 237−253.
(40) Chen, S.; Duhamel, J.; Winnik, M. A. Probing end-to-end cyclization beyond Willemski and Fixmann. *J. Phys. Chem. B* **2011**, *115*, 3289−3302.